

Nonlinear MHD simulations of Quiescent H-mode pedestal in DIII-D and implications for ITER

F. Liu¹, G.T.A. Huijsmans^{2,7}, A. Loarte³, A. M. Garofalo⁴, W. M. Solomon⁴, M. Hoelzl⁵, S. Pamela⁶, M. Becoulet², F. Orain⁵

¹University of Nice Sophia Antipolis, UMR CNRS 7351, Parc Valrose 06108 Nice, France

²CEA, IRFM, F-13108 Saint-Paul-Lez-Durance, France

³ITER Organization, Route de Vinon sur Verdon, CS 90046, 13067 Saint Paul Lez Durance Cedex, France

⁴General Atomics, P.O. Box 85608, San Diego, California 92186-5608, USA

⁵Max Planck Institute for Plasma Physics, 85748 Garching, Germany

⁶CCFE, Culham Science Centre, Abingdon, Oxon, OX14 3DB, UK

⁷Eindhoven University of Technology, Eindhoven, the Netherlands

E-mail contact of main author: feng.liu@iter.org

Abstract. Non-linear MHD simulations of DIII-D Quiescent H-mode (QH-mode) plasmas have been performed with the non-linear MHD code JOREK as a first step towards determining whether the physics mechanisms leading to the QH-mode behaviour would be at work in ITER plasmas and thus whether this confinement regime can be considered as an alternative to the controlled Type I ELMy H-mode for ITER high Q operation. In the nonlinear MHD simulations it is found that low n kink-peeling modes (KPM) are unstable and grow to a saturated level, consistent with the physics picture put forward in linear studies. The features of the dominant MHD modes found in the simulations of the KPM mode, which are due to its toroidal localization caused by the coupling of harmonics, are in good agreement with the observations of the EHO typically present in DIII-D QH-mode experiments. In this work, the non-linear evolution of MHD modes with toroidal mode numbers n from 0 to 10, including both kink-peeling modes and ballooning modes, is investigated through MHD simulations starting from initial conditions either close to the ballooning or the kink-peeling mode limit in the edge stability diagram, both for DIII-D and ITER plasmas. The edge current and pressure at pedestal are key parameters for plasma either saturating to QH-mode regime or ballooning mode dominant regime. The application of non-axisymmetric (NA) magnetic field perturbations effectively selects the toroidal mode number (n=3) on the QH-mode. The preliminary results of the analysis of an ITER Q=10 plasma show the slow growth and saturation of an n=1 kink/peeling mode.

1. Introduction

The QH-mode regime, originally developed at the DIII-D tokamak [1] and investigated in other devices [2-4], has been found to provide high energy confinement without transient energy fluxes to PFCs associated with ELMs. In DIII-D, this operational regime has recently been extended towards conditions suitable for ITER operation such as low torque input [5] and high normalized density operation [6] thus overcoming two important restrictions for its suitability for ITER. In the QH-mode, an edge harmonic oscillation (EHO) is found to provide stationary edge particle transport that replaces the periodic expulsion of particles and energy by ELMs. The EHO is thought to be a saturated external kink/peeling mode driven unstable by edge current and rotation which maintains the edge pressure gradient near but below the ELM instability boundary thus avoiding the triggering of ELMs[7]. One important open question is what causes the plasma to develop either into a QH-mode regime with a saturated external kink mode (EHO) or into a regime with ELMs. For understanding the physics mechanisms of leading to saturation of EHO in DIII-D QH-modes and evaluating whether QH-mode regime is an option for high fusion performance operation at ITER, non-linear MHD simulations of DIII-D QH-mode plasmas have been performed with the non-linear MHD code JOREK[8]. In this paper, a low-n saturated kink-peeling mode which is found in nonlinear MHD simulation, and its physics characteristics including EHO behaviour, density spectrum as well as the comparison with experiment observations will be discussed. The non-linear evolution of MHD modes with toroidal mode numbers n from 0 to 10, including both

kink-peeling modes and ballooning modes, has been investigated through MHD simulations starting from initial conditions either close to the ballooning or the kink-peeling mode limit in the edge stability diagram. The influence of RMP on QH-mode of DIII-D plasma will be discussed. The preliminary results of extrapolation of QH-mode on ITER Q=10 scenario is presented in the last section.

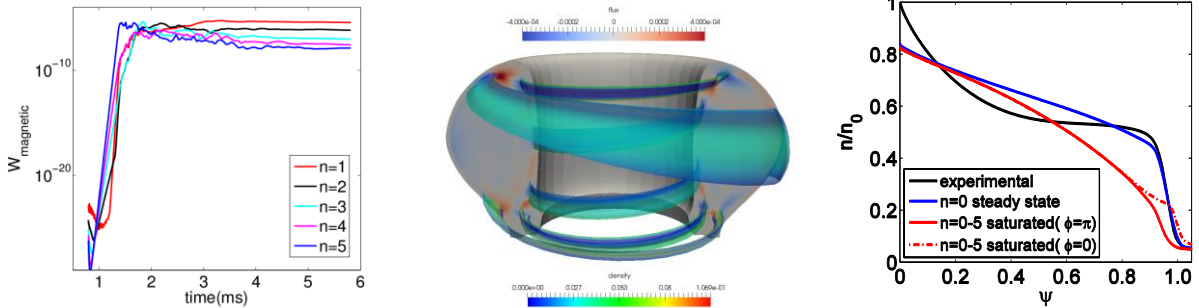


FIG. 1. (a) Time evolution of the perturbed magnetic energy of each harmonic for $n=1-5$ kink peeling mode from the JOREK simulation; (b) 3-D helical structure of the density perturbation for a saturated $n=1-5$ KPM at separatrix; (c) density profiles for an $n = [0-5]$ saturated KPM.

2. Nonlinear MHD simulation of QH-mode plasma

In this work DIII-D QH-mode discharges #145117 has been chosen because it is representative of what could be possible in ITER with the available input torque and externally imposed 3-D field. #145117 is a discharge with $I_p = 1.1\text{MA}$, $B_t = 1.9\text{T}$, counter beam neutral injection at first and then with increasing co-injection to a relevant ITER-like co-torque level and with 3-D non-axisymmetric (NA) magnetic field perturbation applied. The equilibria used in the analysis presented here have been obtained from reconstructions with the EFIT code [9] using the magnetic and profile data for these discharges. Nonlinear MHD simulations of DIII-D shot #145117 including low- n modes ($n=0-5$) performed with the JOREK code assuming ideal wall boundary conditions have been carried out. The effect of 3-D RMP fields is not included here. FIG.1(a) shows the time evolution of the magnetic energy perturbation for the simulation of shot #145117 including toroidal harmonics $n=1-5$. The JOREK simulations show that there is an initial exponentially growing phase of MHD modes. This linear growth phase, which lasts from 0.8ms to 1.3ms is dominated by the medium- n ($n=5$) harmonic. However, due to nonlinear coupling [10] between $n=5$, 4 and 3, the growth of the $n=1$, 2 harmonics is also excited later in the time evolution (at 1.25ms for $n=1$ and 1.35ms for $n = 2$) with non-linear growth rates about 10 times larger than their linear growth rates earlier in the time evolution. After this initial growth phase a non-linear phase starts, from 2ms, where the amplitude of the MHD perturbation saturates into a 3-D stationary state. The dominant mode number of the MHD perturbation changes from $n=5$ in the linear phase down to a predominantly $n=1$ perturbation in the stationary state, with the $n=5$ harmonic decaying to the smallest amplitude in the stationary state. FIG.1(b) shows the 3-D helical structure of the density on a flux surface corresponding to the unperturbed separatrix for the saturated $n=1-5$ kink-peeling mode (KPM). The density perturbation illustrates the 3-D localisation of the KPM at the separatrix in the toroidal and poloidal direction. In these simulations the saturated KPM rotates in the counter clockwise poloidal direction due to the $E \times B$ velocity with a frequency about 1.6kHz. The rotating KPM leads to an oscillation of the plasma at the boundary which corresponds to a displacement of 1.5 cm at the outer mid-plane. FIG.1(c) compares the density profiles at two toroidal phases ($\phi = 0, \pi$) in the presence of a

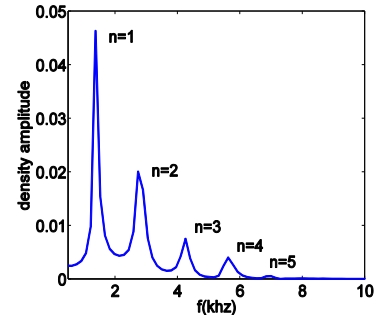


FIG. 2. Density frequency spectrum at normalized $\psi = 0.95$ in outer mid-plane.

saturated $n=0-5$ KPM with the stationary JOREK equilibrium state ($n=0$, blue curve); the experimental density profile (from the time when the EHO is present) is also shown for comparison (black curve). In the simulations it is observed that the presence of a saturated KPM causes a strong additional density loss at the pedestal due to the $E \times B$ convection pattern of the saturated kink-peeling mode. The corresponding frequency spectrum of the density perturbation at the edge of plasma $\psi=0.95$ in mid-plane is plotted in FIG.2. The spectrum shows 5 equally spaced frequencies corresponding to the 5 toroidal harmonics used in the simulations. This indicates a coupling of the toroidal harmonics to form a rotating, toroidally localized structure (as shown in FIG.1(b)). The non-sinusoidal behavior found in the simulations of the KPM mode, which is due to its toroidal localization due to coupling of harmonics, is in good agreement with the observations of the EHO typically present in DIII-D QH-mode experiments [11, 12].

3. Nonlinear identification of QH-mode vs ELMy H-modes

One important open question is what causes the plasma to develop either into a QH-mode regime with a saturated external kink mode [13] or into an H-mode regime with ELMs. The identification of the physics mechanisms that lead to the saturation of the KPM and to the appearance of the edge harmonic oscillation (EHO) in DIII-D QH-modes will allow us to evaluate the possibility of high fusion performance ITER operation in this operational mode. For this purpose, the non-linear evolution of MHD modes with toroidal mode numbers n from 0 to 10, including toroidal modes typical for both kink-peeling modes and ballooning modes, have been investigated through MHD simulations with initial conditions corresponding to the experimental data #145117 and by varying both pedestal pressure and edge current either close to the ballooning or the kink-peeling mode to obtain the limit of either the EHO or Type I ELMs in the edge stability diagram.

3.1 Nonlinear simulation of $n=0-10$ with experimental equilibrium

The time evolution of the toroidal harmonics $n=1-10$ of the magnetic energy perturbation for the JOREK simulation of the original DIII-D equilibrium in FIG.3(a) shows that there is an initial exponentially growth phase of MHD modes. This linear growth phase, which lasts from 0.8ms to 1.2ms is dominated by the high- n ($n=10$) harmonics. However, due to nonlinear coupling between the harmonics $n=5-10$, the growth of the $n=1-4$ harmonics is also non-linearly excited later in the time evolution after 1.0ms with non-linear growth rates about 10 times larger than their linear growth rates earlier in the time evolution. The system reaches a 3-D quasi-stationary saturated state at about 1.2ms, as clearly shown in FIG.3(b). The dominant mode numbers of the MHD perturbation in the stationary state are low- n harmonics $n=1, 2, 3$, particularly the $n=2$ mode. Its energy level is the highest and dominant through the stationary state. It has been observed that even harmonics ($n=2,4,6$) have higher magnitude than odd harmonics in some QH-mode experiments [12]. For higher n harmonics such as $n=9, 10$, the amplitude of its energy quickly decays to low level once the system reaches stationary state. This time evolution of the energy of the modes shows that the plasma is dominated by an EHO associated with a saturated low- n kink/peeling mode [11], which is typical of the QH-mode.

The density profiles for two toroidal phases ($\phi = 0, \pi$) in the stationary state for $n=0-10$ modes together with that of the stationary JOREK equilibrium state ($n=0$, blue curve) are shown in FIG.3(c), compared with the initial experimental density profile (black curve). The density with the presence of the dominant kink/peeling mode and residual ballooning modes decreases by more than 30% at pedestal. The different density profiles at different toroidal phases also indicate that the density profile has an oscillation at the edge of the plasma and causes a displacement of about 1.5cm of the density profile.

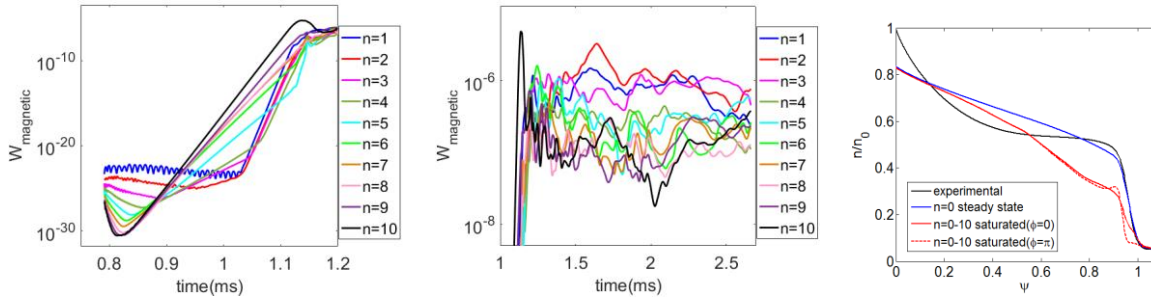


FIG. 3. Time evolution of the perturbed magnetic energy of each harmonic for $n=1-10$ modes at linear growth phase(a) and at saturation phase(b) for the JOREK simulations; (c) Density profiles for $n = [0-10]$ at saturation phase.

The simulations of JOREK with toroidal harmonics $n=0-10$ with the equilibrium QH-mode plasma of DIII-D indicate that there are, initially, both unstable kink/peeling and ballooning modes in the edge of plasma. Although high- n modes have larger growth rates in the linear growth phase, the low- n modes (associated with EHO) dominate the system with high energy saturated level once the system reaches the stationary state.

3.2 Nonlinear simulation of $n=0-10$ with increased pedestal pressure

In order to understand what causes the plasma to develop either into a QH-mode regime with a saturated external kink mode (EHO) or into a regime with ELMs, the edge current and height of pressure pedestal of QH-mode plasma equilibrium of DIII-D have been varied and simulated including toroidal harmonics $n=0-10$, as shown in the stability diagram in FIG.4(a): the black star represents the experimental equilibrium of the DIII-D QH-mode plasma #145117, the red star represents an equilibrium with higher pedestal pressure than the experiment, the green star represents an equilibrium with reduced edge current, and the yellow star represents an equilibrium with both reduced edge current and increased pedestal pressure compared to the experiment. The nonlinear simulations including $n=0-10$ modes introduced above shows that the experimental equilibrium (black star in FIG.4.(a)) is in a kink-peeling mode (EHO) dominant region. However including diamagnetic flow effects into the simulations with $n=0-5$ toroidal harmonics makes the edge plasma to be MHD stable. The physics of the nonlinear MHD stability of QH-mode plasmas including the effect of diamagnetic flow is still under investigation. In this paper the effect of diamagnetic flow is not included but we note that its inclusion could affect the degree of the modelled MHD instability in our simulations.

The equilibrium with 30% higher pressure pedestal (represented as red star in FIG.4(a)) has been obtained in JOREK by modifying the diffusion coefficients, heat conductivity at pedestal, particle source and heating source. Though the current profile is also slightly modified due to the self-consistent inclusion of the pressure in the equilibrium, this change is negligible. The time evolution of magnetic energy for toroidal harmonics $n=1-10$ for this higher pressure pedestal equilibrium during the linear growth phase is similar to that of the simulation with the experimental equilibrium, with high- n modes having the largest growth rates and dominating the linear growth phase, so that here only the time evolution of magnetic energy from reaching stationary state 1ms to 1.35ms is shown in FIG.4(b). After ~ 1.1 ms the level of $n=9-10$ modes decay rapidly and gives rise to dominant $n=2-3$ at the beginning of stationary state where $n=2$ becomes dominant from 1.25ms with the highest magnetic energy level, followed by $n=3$; the magnetic energy level of high- n modes $n=9-10$ decays to the lowest amplitude in the saturated phase. The density profiles for $n=0-10$ during stationary state is shown in FIG.4(c). The oscillation at different toroidal phases at the edge of plasma causes a displacement about 1.5cm, which is similar with the case of simulation with experimental equilibrium.

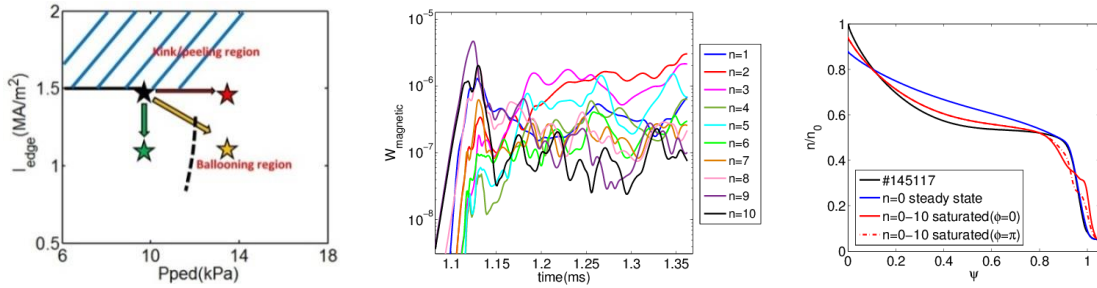


FIG. 4. (a) Sketch of the stability diagram of the equilibria studied with a range of edge current and pedestal pressure levels; (b) Perturbed magnetic energy evolution of $n=1-10$ modes for the JOREK simulations with increased pressure at pedestal; (c) Density profiles for $n = [0-10]$ during saturation phase at $t=1.35\text{ms}$.

The behaviour of plasma indicates that QH-mode associated with low- n modes dominate the system more than ballooning modes (high- n modes) in the plasma with 30% higher pressure at pedestal and the same level of pedestal current. The initial burst with a fast growth of the $n=9, 10$ harmonics is very similar to that observed in simulations of ELMs [14]. However, here the duration of the initial ELM-like burst is only $50\mu\text{s}$. Due to the non-linear coupling, the low- n harmonics are excited, typical of a QH mode state. The reduction of the edge density is smaller in this case compared to the experimental case, this is thought to be due to the large power and particle sources required to obtain this equilibrium.

3.3 Nonlinear simulation of $n=0-10$ with reduced edge current

The current profiles for the equilibrium with reduced edge current density represented as the green star in FIG.4(a) is shown in FIG.5(a) (red curve) compared with the equilibrium for the current density of the DIII-D QH-mode plasma (black curve) and has about 30% lower edge current compared to the original equilibrium. It should be noted that only the edge current density is reduced in this study, the pressure profile in the equilibrium remains unchanged compared to the original DIII-D equilibrium.

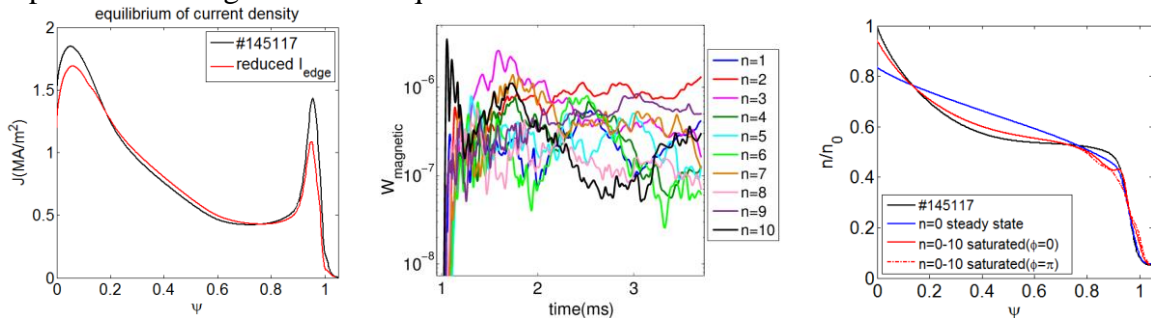


FIG. 5. (a) Current profiles. Initial equilibrium current profile of experimental data (black curve) and the equilibrium of reduced edge current profile (red curve); (b) The perturbed magnetic energy evolution of $n=1-10$ modes during saturated phase for the JOREK simulations with the reduced current equilibrium; (c) Density profiles for $n = [0-10]$ during saturated phase with reduced edge current equilibrium.

The time evolution of the perturbed magnetic energy of the $n=1-10$ toroidal harmonics from the initial growth to steady-state for the JOREK simulations of the equilibrium with lower edge current is shown in FIG.5(b). Also this case shows an initial ELM-like behavior with a large energy amplitude $n=10$ ballooning mode decaying to a state dominated by a $n=2$ KPM. In this case $n=2$ is the dominant mode in the saturated state but with a reduced amplitude compared to the case with the higher edge current. The density profile of the simulation including toroidal harmonics $n=0-10$ with reduced edge current density is shown in FIG.5(c). Due to the lower mode amplitude, the density has only a very minor loss at pedestal and the

profiles at different toroidal phase are very similar showing that the scale of density oscillation at the edge is also small.

3.4 Nonlinear simulation of $n=0-10$ with reduced edge current and increased pedestal pressure

For further studying the identification boundary of edge parameters leading to the QH-mode or ELMs, the simulation including $n=1-10$ toroidal harmonics with the equilibrium, represented as yellow star in FIG.4(a), which has a lower edge current profile as in FIG.5(a) red curve, and 30% higher pedestal pressure than the experimental one has been investigated. FIG.6(a) shows the time evolution of magnetic energy of each toroidal harmonic $n=1-10$ during the time 1ms to 2.5ms from JOEKE simulation. Early in the simulation strong ELM-like behavior is shown by the $n=10$ mode which has large amplitude, multiple bursts and an increased amplitude compared to the lower pedestal pressure case. From 1ms onwards the ballooning mode $n=10$ decays rapidly down to a low level, very similar with the case of equilibrium with reduced edge current but the same value of pedestal pressure as the experiment. After the magnetic energy level of $n=10$ mode decays, the amplitude level of $n=9$ mode slowly rises and then dominates the stationary state from 1.5ms, while $n=2$ becomes the secondary mode. After a long time evolution, the amplitude of energy $n=10$ ballooning slowly rises and dominates the stationary system. This is different from any of the other cases presented in this paper where the EHO is dominant in the stationary plasma. The pressure profiles of $n=0-10$ harmonics in stationary state at the edge ($\psi=0.6-1.0$) shown in FIG.6(b) has about 25% pedestal loss due ballooning mode. FIG.6(c) shows a contour plot of the flux perturbation in poloidal plane during the saturated phase. The magnetic perturbation has a very clear ballooning mode structure localized on the edge of plasma. Therefore the plasma with lower edge current and higher pedestal pressure shows a behaviour clearly more typical for ballooning modes than QH mode. However, the precise identification of the EHO versus the ELMs boundary is not yet clear. Recently it has been shown that diamagnetic flows need to be considered to obtain a regime with repetitive ELMs[15]. The influence of diamagnetic flows on the ELMy H-mode versus QH mode regime will be considered in future work.

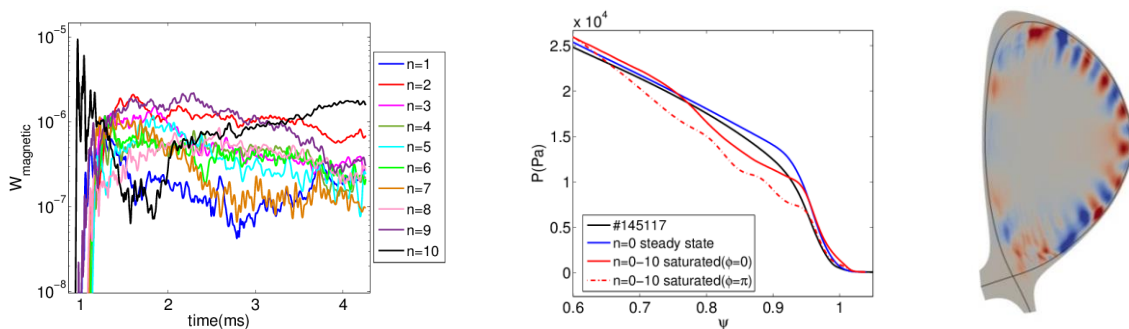


FIG.6. JOEKE simulations including $n=0-10$ modes with the reduced edge current and higher pedestal pressure equilibrium. (a) Time evolution of the magnetic energy during saturated phase; (b) pressure profiles for $n = [0-10]$ in saturated phase (c) contour plot of the poloidal flux perturbation in saturated phase with separatrix(black curve).

4. Influence of RMP on QH-mode plasma

In this section, the effect of $n=3$ RMPs with $I_{\text{coil}}=4\text{kA}$ are included in the JOEKE simulations of the QH-mode plasma of DIII-D #145117. The plasma response to RMP in the JOEKE simulation including toroidal harmonics $n=0-5$ with RMPs, occurs in a very different way than without RMPs. FIG.7(a) shows the time evolution of magnetic energy for $n=1-5$ with RMPs from the JOEKE simulation. The initial linear growth phase starts from a higher initial state due to the externally applied $n=3$ field. It is observed that the $n=1,2,4,5$ grow slowly and to a much smaller saturation amplitude. The energy of $n=3$ saturates at a much higher level,

with a value of 5.5×10^{-6} . The large $n=3$ amplitude appears to suppress the other toroidal harmonics; the energy of the other modes remains at much lower stationary level. In contrast, the time evolution of $n=1-5$ without RMPs shown in FIG.1(a) shows that the plasma behaves totally differently as in that case the energy of toroidal harmonics $n=1-5$ starts to grow with $n=5$ being dominant in the linear growth phase and then decreasing to a lower level as the lower ($n=1$) KPM becomes dominant in the saturated phase. The Poincare plot at the plasma edge $\psi=[0.7-1.0]$ at FIG.7(b) shows the edge ergodic islands due to RMP $n=3$ mode. It should be noted that the saturation amplitude of the $n=3$ mode is determined by the $n=3$ kink-peeling mode which is comparable to the amplitude of the $n=3$ when the RMP perturbation is not applied.

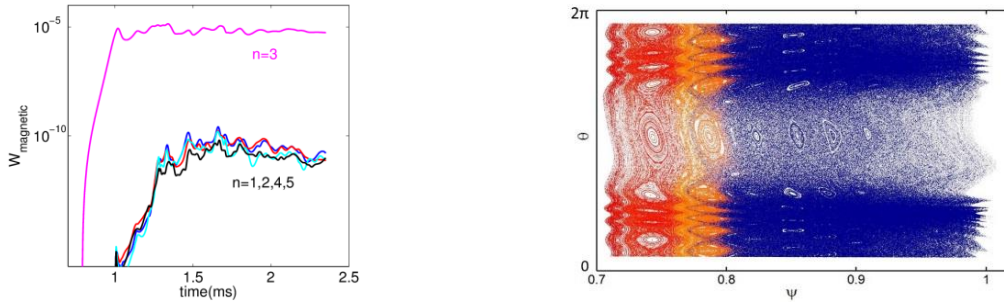


FIG.7.(a)Time evolution of the perturbed magnetic energy of each harmonic for $n=1-5$ with RMP;(b)Poincare plot of magnetic topology in (ψ, θ) coordinates.

5. Extrapolation of ITER Q=10 scenario on QH-mode with JOREK

The low- n stability of an ITER baseline scenario $Q=10$ with plasma current $I=15\text{MA}$, magnetic field $B=5.3\text{T}$, major radius $R=6.2\text{m}$, minor radius $a=2.0\text{m}$ [16] has been analyzed with respect to the access to a possible QH-mode regime. The equilibrium of ITER plasma is generated by CORSICA [17]. Preliminary results of the simulations including toroidal harmonics $n=0-1$ and the ITER resistive wall (the vacuum vessel) by using JOREK-STARWALL[18] is obtained. The equilibrium with a pedestal pressure of 120kPa is unstable to a slow growing $n=1$ kink-peeling mode with growth rate $\sim 1 \text{ ms}^{-1}$ when the realistic wall resistivity of $\eta=1.0 \times 10^{-6} \Omega\text{m}$. The growth rate of the mode is increasing with the increase of wall resistivity. In the non-linear phase, the kink-peeling mode saturates into a quasi-stationary state with a relatively small amplitude density oscillation of $\sim 1\text{cm}$ at the plasma boundary. The plasma density at separatrix in 3-D structure and the potential in the resistive wall during the saturation phase of the $n=1$ mode show (see FIG.(8)) the characteristic kink/peeling mode structure localized at the edge of plasma.

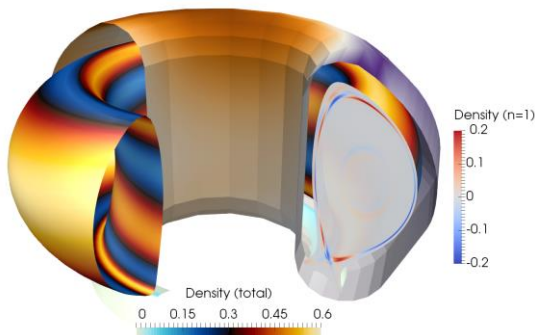


FIG.8.(a) 3-D density structure at the separatrix and resistive wall potential of a $n=1$ saturated kink mode in ITER Q=10 scenario

6. Conclusion

In the nonlinear MHD simulations of DIII-D QH-mode plasmas with low- n harmonics $n=0-5$, kink/peeling modes have been found to grow exponentially in the linear phase and then nonlinearly saturate into a new 3-D stationary EHO phase. The saturated KPM mode leads to

oscillations in the edge magnetic field, position of the plasma boundary and plasma density with the typical multi-harmonic content associated with the EHO in QH-mode plasmas observed experimentally in magnetics and fast reflectometer measurements.

Variations of the pedestal profiles of the initial equilibria have shown that at increased pedestal pressure and lower pedestal current, the saturated state of the EHO with a low- n kink-peeling mode does not develop. Instead, there is an initial ELM-like event followed by stationary phase with a $n=9-10$ ballooning mode. Reducing the pedestal current at constant pedestal pressure reduces the amplitude of the saturated kink-peeling mode, leading to significantly lower losses of the pedestal density. The simulations show the edge plasma current required to drive an EHO (stationary QH-mode) is not only simply that required to linearly or non-linearly destabilize a low- n kink-peeling mode. In addition the amplitude of the mode needs to be large enough to cause a significant transport of density to obtain a stationary state. The application of an external non-axisymmetric field perturbation (RMP) is very effective in selecting the toroidal mode number of the saturated QH-mode. The growth of the kink-peeling mode is not due to non-linear interaction of higher- n toroidal harmonics but starts from the applied external field perturbation. These simulations suggest that the application of an $n=3$ mode effectively stabilises the other toroidal harmonics. Preliminary JOREK simulation results of ITER $Q=10$ plasma shows that the pedestal currents are large enough to destabilise an $n=1$ kink-peeling mode, leading to a saturated kink-peeling mode. Whether the amplitude of the saturated state is large enough to cause a significant density loss similar to that observed in the DIII-D QH-mode simulations is the subject of on-going simulations with more harmonics.

This work was supported in part by the US Department of Energy under DE-FC02-04ER54698 and DE-AC03-09CH11466.

The views and opinions expressed herein do not necessarily reflect those of the ITER Organization.

Reference

- [1] Burrell K.H. et al., Bull. Am. Phys. Soc. **44** (1999) 127
- [2] Suttrop W. et al., Nucl. Fusion **45** (2005) 721
- [3] Sakamoto Y. et al Plasma Phys. Control. Fusion **46** (2004) A299
- [4] Oyama N. et al., Nucl. Fusion **45** (2005) 871
- [5] Garofalo A.M. et al., Nucl. Fus. **51** (2011) 083018
- [6] Solomon W. et al., Phys. Rev. Lett. **113** (2014) 135001
- [7] Snyder, P.B. et al., Nucl. Fusion **47** (2007) 961
- [8] Huysmans G.T.A. et al., Nucl. Fusion. **47** (2007) 659
- [9] Lao, L. et al., Nucl. Fusion 30 (1990) 1035
- [10] Krebs I. et al., Physics of Plasmas, **20** (2013) 082506
- [11] Liu F. et al., Nucl. Fusion **55** (2015) 113002
- [12] Burrell K.H. et al., Nucl. Fusion **53** (2013) 073038
- [13] Loarte A. et al, Nucl. Fusion **47** (2007) S203
- [14] Huijsmans G.T.A. et al., Nucl. Fusion **53** (2013) 123023
- [15] Orain F. et al., Plasma Physics and Controlled Fusion **57** (2014) 014020
- [16] T. Casper et al Nucl. Fusion **54** (2014) 013005
- [17] Crotinger J.A. et al., LLNL Report UCRL-ID-126284, NTIS (1997) #PB2005-102154
- [18] Hoelzl M. et al., Journal of Physics: Conference Series, **401** (2012) 012010